Highly efficient nonradiative energy transfer mediated light harvesting in water using aqueous CdTe quantum dot antennas

Evren Mutlugun,[1] Olga Samarskaya,[1] Tuncay Ozel,[1] Neslihan Cicek,[1] Nikolai Gaponik,[2] Alexander Eychmüller,[2] and Hilmi Volkan Demir[1,*]

[1]*Department of Physics, Department of Electrical and Electronics Engineering, UNAM — National Nanotechnology Research Center, Bilkent University, 06800, Ankara, Turkey*
[2]*Physical Chemistry, TU Dresden, Bergstr.66b, 01062, Dresden, Germany*
**volkan@bilkent.edu.tr*

Abstract: We present light harvesting of aqueous colloidal quantum dots to nonradiatively transfer their excitonic excitation energy efficiently to dye molecules in water, without requiring ligand exchange. These as-synthesized CdTe quantum dots that are used as donors to serve as light-harvesting antennas are carefully optimized to match the electronic structure of Rhodamine B molecules used as acceptors for light harvesting in aqueous medium. By varying the acceptor to donor concentration ratio, we measure the light harvesting factor, along with substantial lifetime modifications of these water-soluble quantum dots, from 25.3 ns to 7.2 ns as a result of their energy transfer with efficiency levels up to 86%. Such nonradiative energy transfer mediated light harvesting in aqueous medium holds great promise for future quantum dot multiplexed dye biodetection systems.

OCIS codes: (230.5590) Quantum-well, -wire and -dot devices; (160.2540) Fluorescent and luminescent materials; (160.4670) Optical materials; (160.4760) Optical properties; (260.2160) Energy Transfer; (160.1435) Biomaterials

References and links

1. A. Georgi, C. Mottola-Hartshorn, A. N. Warner, B. Fields, and L. B. Chen, "Detection of individual fluorescently labeled reovirions in living cells," Proc. Natl. Acad. Sci. U.S.A. **87**(17), 6579–6583 (1990).
2. Y. Li, Y. T. H. Cu, and D. Luo, "Multiplexed detection of pathogen DNA with DNA- based fluorescence nanobarcodes," Nat. Biotechnol. **23**(7), 885–889 (2005).
3. K. Bacia, S. A. Kim, and P. Schwille, "Fluorescence cross-correlation spectroscopy in living cells," Nat. Methods **3**(2), 83–89 (2006).
4. C. Fang, A. Agarwal, K. D. Buddharaju, N. M. Khalid, S. M. Salim, E. Widjaja, M. V. Garland, N. Balasubramanian, and D. L. Kwong, "DNA detection using nanostructured SERS substrates with Rhodamine B as Raman label," Biosens. Bioelectron. **24**(2), 216–221 (2008).
5. H. Tokudome, Y. Yamada, S. Sonezaki, H. Ishikawa, M. Bekki, K. Kanehira, and M. Miyauchi, "Photoelectrochemical deoxyribonucleic acid sensing on a nanostructured TiO_2 electrode," Appl. Phys. Lett. **87**(21), 213901 (2005).
6. B. O'Reagen, and M. Grätzel, "A low-cost, high-efficiency solar cell based on dye-sensitized colloidal TiO_2 films," Nature **353**(6346), 737–740 (1991).
7. S. L. Li, K. J. Jiang, K. F. Shao, and L. M. Yang, "Novel organic dyes for efficient dye-sensitized solar cells," Chem. Commun. (Camb.) **26**(26), 2792–2794 (2006).
8. E. Mutlugün, S. Nizamoglu, and H. V. Demir, "Highly efficient nonradiative energy transfer using charged CdSe/ZnS nanocrystals for light-harvesting in solution," Appl. Phys. Lett. **95**(3), 033106 (2009).
9. W. W. Yu, E. Chang, R. Drezek, and V. L. Colvin, "Water-soluble quantum dots for biomedical applications," Biochem. Biophys. Res. Commun. **348**(3), 781–786 (2006).
10. S. Kim, and M. G. Bawendi, "Oligomeric Ligands for Luminescent and Stable Nanocrystal Quantum Dots," J. Am. Chem. Soc. **125**(48), 14652–14653 (2003).
11. M. Grabolle, M. Spieles, V. Lesnyak, N. Gaponik, A. Eychmüller, and U. Resch-Genger, "Determination of the Fluorescence Quantum Yield of Quantum Dots: Suitable Procedures and Achievable Uncertainties," Anal. Chem. **81**(15), 6285–6294 (2009).
12. N. Gaponik, D. V. Talapin, A. L. Rogach, K. Hoppe, E. V. Shevchenko, A. Kornowski, A. Eychmüller, and H. Weller, "Thiol-Capping of CdTe nanocrystals: An alternative to organometallic synthetic routes," J. Phys. Chem. B **106**(29), 7177–7185 (2002).

#124054 - $15.00 USD Received 9 Feb 2010; revised 23 Apr 2010; accepted 28 Apr 2010; published 7 May 2010

13. A. L. Rogach, T. Franzl, T. A. Klar, J. Feldmann, N. Gaponik, V. Lesnyak, A. Shavel, A. Eychmüller, Y. P. Rakovich, and J. F. Donegan, "Aqueous synthesis of thiol-capped CdTe nanocrystals: State-of-the-art," J. Phys. Chem. C **111**(40), 14628–14637 (2007).
14. T. Förster, "Zwischenmolekulare Energiewanderung und Fluoreszenz," Ann. Phys. **437**(1-2), 55–75 (1948).
15. A. R. Clapp, I. L. Medintz, J. M. Mauro, B. R. Fisher, M. G. Bawendi, and H. Mattoussi, "Fluorescence resonance energy transfer between quantum dot donors and dye-labeled protein acceptors," J. Am. Chem. Soc. **126**(1), 301–310 (2004).
16. D. M. Willard, and A. Van Orden, "Quantum dots: Resonant energy-transfer sensor," Nat. Mater. **2**(9), 575–576 (2003).
17. I. L. Medintz, A. R. Clapp, F. M. Brunel, T. Tiefenbrunn, H. T. Uyeda, E. L. Chang, J. R. Deschamps, P. E. Dawson, and H. Mattoussi, "Proteolytic activity monitored by fluorescence resonance energy transfer through quantum-dot-peptide conjugates," Nat. Mater. **5**(7), 581–589 (2006).
18. S. Sadhu, and A. Patra, "Composition effects on quantum dot-based resonance energy transfer," Appl. Phys. Lett. **93**(18), 183104 (2008).
19. P. S. Chowdhury, P. Sen, and A. Patra, "Optical properties of CdS nanoparticles and the energy transfer from CdS nanoparticles to Rhodamine 6G," Chem. Phys. Lett. **413**(4-6), 311–314 (2005).
20. T. Pons, I. L. Medintz, M. Sykora, and H. Mattoussi, "Spectrally resolved energy transfer using quantum dot donors: Ensemble and single-molecule photoluminescence studies," Phys. Rev. B **73**(24), 245302 (2006).
21. E. Alphandery, L. M. Walsh, Y. Rakovich, A. L. Bradley, J. F. Donegan, and N. Gaponik, "Highly efficient Förster resonance energy transfer between CdTe nanocrystals and Rhodamine B in mixed solid films," Chem. Phys. Lett. **388**(1-3), 100–104 (2004).
22. X. Y. Wang, Q. Maa, Y. B. Lia, B. Li, X. G. Su, and Q. H. Jin, "Studies on fluorescence resonance energy transfer between dyes and water-soluble quantum dots," Can. J. Anal. Sci. Spectrosc. **50**, 141–146 (2005).
23. J. Li, F. Mei, W. Y. Li, X. W. He, and Y. K. Zhang, "Study on the fluorescence resonance energy transfer between CdTe QDs and butyl-rhodamine B in the presence of CTMAB and its application on the detection of Hg(II)," Spectrochimica Acta Part A **70**(4), 811–817 (2008).
24. Q. Chen, Q. Ma, Y. Wan, X. Su, Z. Lin, and Q. Jin, "Studies on fluorescence resonance energy transfer between dyes and water-soluble quantum dots," J. Biolumin. Chemilumin. **20**(4-5), 251–255 (2005).
25. A. R. Clapp, I. L. Medintz, and H. Mattoussi, "Förster resonance energy transfer investigations using quantum-dot fluorophores," Chem. Phys. Chem **7**(1), 47–57 (2006).
26. J. R. Lakowicz, *Principles of Fluorescence Spectroscopy* (New York: Springer,2006).
27. V. K. Komarala, A. L. Bradley, Y. P. Rakovich, S. J. Byrne, Y. K. Gun'ko, and A. L. Rogach, "Surface plasmon enhanced Förster resonance energy transfer between the CdTe quantum dots," Appl. Phys. Lett. **93**(12), 123102 (2008).
28. S. Chanyawadee, R. T. Harley, M. Henini, D. V. Talapin, and P. G. Lagoudakis, "Photocurrent Enhancement in Hybrid Nanocrystal Quantum-Dot p-i-n Photovoltaic Devices," Phys. Rev. Lett. **102**(7), 077402 (2009).

1. Introduction

Today dye molecules are widely used in molecular biology. They offer several benefits including good biocompatibilty, high quantum yield, and reasonable photostability. Some of their common applications include biolabeling, biodetection, and spectroscopy [1–3]. Also, their small size of only a few nanometers allows for their use in molecular-level detection systems (e.g., in double stranded deoxyribonucleic acid (DNA), which is not possible with larger size biotags [4, 5]). Despite these unique advantages, organic dyes, suffer one main drawback that they cannot be efficiently pumped over a wide spectral range beyond their characteristically narrow absorption spectra (for example, see Fig. 1a for Rhodamine B). This limits their use in some important applications that require broader spectral operation including spectral multiplexing (in which various dyes can simultaneously be pumped using a single source). Also for dyes, spectral extension of their optical absorption is important in photovoltaic applications where dyes are used as sensitizers [6]. The dye sensitized solar cells require a wide spectral response for an enhanced efficiency, but broadening of the absorption spectra of dyes generally necessitates complicated chemical modifications [7].

To address these problems, by using semiconductor quantum dot nanocrystals, nonradiative Förster-type resonance energy transfer (FRET) can be employed to enable light harvesting at optical wavelengths beyond the absorption range of dye molecules, and thus to effectively extend their absorption. Such nanocrystals feature high-efficiency, Gaussian-like distributed emission along with high tunability of absorption/emission characteristics, which make them good candidates as donors for light harvesting, as we have shown in our previous work [8]. However, the solubility of such donor quantum dots in aqueous media is a critical issue to provide biocompatibility and enable biological applications [9]. To be dissolved in water, the ligand exchange of nanocrystals is an alternative, but this comes at a cost of

#124054 - $15.00 USD Received 9 Feb 2010; revised 23 Apr 2010; accepted 28 Apr 2010; published 7 May 2010

significantly decreased quantum efficiency [10]. On the other hand, aqueous CdTe quantum dots provide as-synthesized water solubility and high quantum yield [11], and their synthesis has already been studied and well established [12, 13]. For these reasons, aqueous CdTe is one of the best candidates as light-harvesting antenna in water. However, such as-synthesized aqeuous quantum dots have not been investigated or demonstrated for light harvesting in water to date, although this is of ciritical importance for spectrally extended bioimaging and biolabeling applications.

Nonradiative transfer of the electronic excitation energy from electronically excited donor molecules to optically luminescent acceptor molecules in close proximity was first discussed by Theodor Förster in 1948 [14]. Till date FRET has been extensively studied in different FRET pairs of dyes and nanocrystals for various applications [15–20] (also including CdTe nanocrystals [21–25]). Although these previous reports have demonstrated FRET mechanism using such a large variety of FRET pairs, light harvesting based on FRET using aqueous nanocrystals has not been reported. In the previous work of our group, light harvesting of organic nanocrystals synthesized in apolar solvents was investigated; this, however, undesirably came at the cost of requiring ligand exchange. Avoiding the need for the ligand exchange, the light harvesting factor of as-synthesized aqueous nanocrystals and their systematic tuning and control in aqueous medium for light harvesting have not been reported.

In this paper, different than the prior works of our group and the others, we propose and demonstrate light harvesting of aqueous colloidal CdTe quantum dots to nonradiatively transfer their excitonic excitation energy efficiently to dye molecules in water, and present systematic tuning and control of their light harvesting activity in aqueous medium, without the need for ligand exchange. We investigated the effects of Förster radius of these aqueous nanocrystals on modifying their lifetimes and controlling their light harvesting factor in water. We studied the operation of these CdTe nanocrystal donors, serving as optical antennas for acceptor Rhodamine B molecules, with their steady state photoluminescence (SSPL) spectroscopy and further investigated and analyzed their significantly modified photoluminescence decay kinetics for light harvesting with their time resolved photoluminescence (TRPL) spectroscopy.

With acceptor to donor (A/D) concentration ratio varied in water, we controlled the light harvesting factor of the donor CdTe quantum dots, with their substantial lifetime modifications as a result of the nonradiative energy transfer with high efficiency levels (up to 86%). We further analyzed the controlled change in the lifetime of the acceptor molecules and investigated the resulting trend of increasing energy transfer efficiency versus decreasing light harvesting enhancement of the acceptor emission with the increased A/D concentration ratio, discussing the fundamental tradeoffs and practical feasibility of nonradiative energy transfer assisted light harvesting operation with reasonable efficiency and enhancement.

2. Experimental characterization, analyses, and results

In this work we colloidally synthesized aqueous CdTe quantum dots in two different sizes to study the effect of Förster radius on the energy transfer efficiency and light harvesting activity. Our synthesis procedure follows the method previously described in detail in references 11 and 12. In our synthesis, 4.59 g of $Cd(ClO_4)_2x6H_2O$ is dissolved in 0.5 l of Milli-Q water in 1 l three-neck reaction flask. 1.33 g of TGA is added to the mixture, which turns into milky appearance. The pH of this mixture is then increased to 11.8 – 12.0 by dropwise addition of NaOH upon vigorous stirring. After this step, the reaction mixture becomes clear or slightly turbid. To prepare tellurium precursor, 0.8 g of Al_2Te_3 is transferred into a small three-neck flask in the glove box and then deaerated by passing Ar for 50-60 min in the setup. 10 ml of deaerated 0.5 M H_2SO_4 is slowly poured into Al_2Te_3 lumps to produce H_2Te gas, which is carried by a slow Ar flow and bubbled through the mixture containing cadmium precursor for 40-50 min. The resulting red-black mixture is refluxed at 100°C to obtain the desired nanocrystal size. The reaction mixture is then cooled to room temperature and filtered. The CdTe quantum dots are finally separated by size selective precipitation.

#124054 - $15.00 USD Received 9 Feb 2010; revised 23 Apr 2010; accepted 28 Apr 2010; published 7 May 2010

Figure 1a shows the optical absorption spectra of these differently sized CdTe quantum dot donors carefully chosen by size selection, along with that of Rhodamine B acceptor molecules in water. Figure 1b depicts the photoluminescence spectra of these CdTe quantum dots selectively chosen to emit at the peak emission wavelengths of 525 nm and 552 nm (corresponding to 2.04 nm and 2.98 nm in size, respectively), presented here along with the emission and absorption spectra of the acceptor dye molecules alone to show the spectral overlap. Here the absorbance measurements were taken using Cary UV-VIS spectrophotometer and the photoluminescence measurements were carried out using Cary Eclipse fluorescence spectrophotometer.

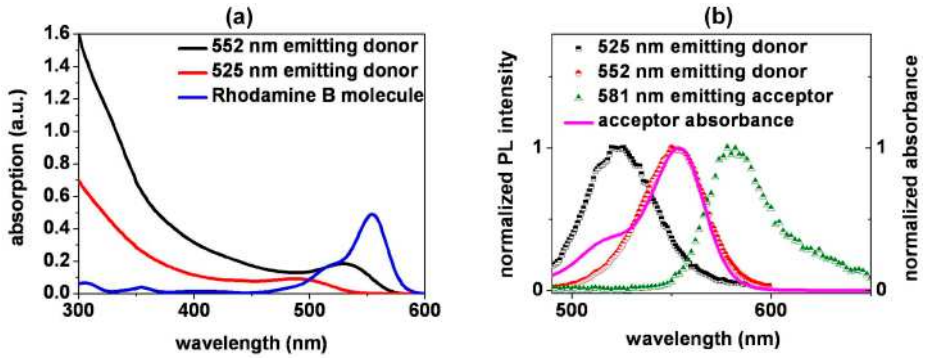

Fig. 1. (a) Absorbance spectra of the two differently sized aqueous CdTe nanocrystal quantum dots (emitting at 552 and 525 nm) together with that of the Rhodamine B dye molecules. (b) Normalized photoluminescence spectra of our aqueous CdTe quantum dots (donors) selectively chosen to emit at the peak wavelengths of 525 nm and 552 nm, along with the emission and absorption spectra of the Rhodamine B molecules (acceptors). The donors emitting at 552 nm provide a better spectral match to the electronic structure of these acceptors.

Förster radius, which is defined as the distance between the donor and acceptor molecules yielding a 50% efficient energy transfer, is given by Eq. (1)

$$R_0 = 0.211(\kappa^2 n^{-4} Q_D J(\lambda))^{1/6} \quad (1)$$

where κ^2 is the dipole orientation factor; n is the refractive index of the medium; Q_D is the quantum efficiency of the donor; $J(\lambda)$ is the overlap integral of the donor emission spectrum and the acceptor absorption spectrum; and R_o is expressed in terms of Angstroms (Å) [26]. Figure 1b is used to calculate the spectral overlap integrals $J(\lambda)$, which leads to 5.5×10^{15} and 9.2×10^{15} for the donor quantum dots emitting at 525 nm and 552 nm, respectively. Subsequently, the quantum efficiencies of the donor molecules are experimentally measured to be 10% and 54% for 525 nm emitting and for 552 nm emitting dots, respectively using Rhodamine 6G as the reference dye. This difference in the quantum efficiency is commonly observed for this type of nanocrystals; their quantum efficiencies increase with increasing size, which is inevitable for such only core structures. Using Eq. (1), the Förster radii calculated are $R_o = 4.7$ and $R_o = 6.7$ nm, for 525 nm and 552 nm quantum dots, respectively. This difference in the Förster radius comes both from the spectral overlap and quantum efficiency difference. Based on this observation, the quantum dot donors emitting at 552 nm are found to have a wider Förster interaction range and thus to be a better optimized match to the acceptor dyes, compared to 525 nm emitting dots,

2.1 Steady State Photoluminescence (SPPL) measurements

To observe FRET, we first performed SSPL measurements (with optical excitation at 375 nm) while adding controlled amounts of acceptor molecules into the aqueous donor solution, thus changing A/D ratio in increments. Figure 2a presents SSPL spectra for our CdTe quantum

#124054 - $15.00 USD Received 9 Feb 2010; revised 23 Apr 2010; accepted 28 Apr 2010; published 7 May 2010

dots emitting at 552 nm used as the donors and Fig. 2b shows the results of the same measurements repeated using 525 nm emitting dots as the donors, both starting with the same concentration levels and changing A/D concentration ratio in an identical manner in water. In this steady state characterization, optical excitation is chosen at 375 nm to be consistent with that of the time resolved measurements that use a 375 nm laser diode pump. It is worth noting that our donor molecules are optically well excited at 375 nm, while this excitation wavelength is out of the absorption range of the acceptor molecules (Fig. 1a). Here the concentrations of the donors (without acceptors) and acceptors (without donors) used in Fig. 1a correspond to the same starting points of Fig. 2 before adding the acceptor molecules into the aqueous donor solution. As A/D concentration ratio is increased, we clearly observe simultaneously the quenching of donor emission and the enhancement of acceptor emission in increments.

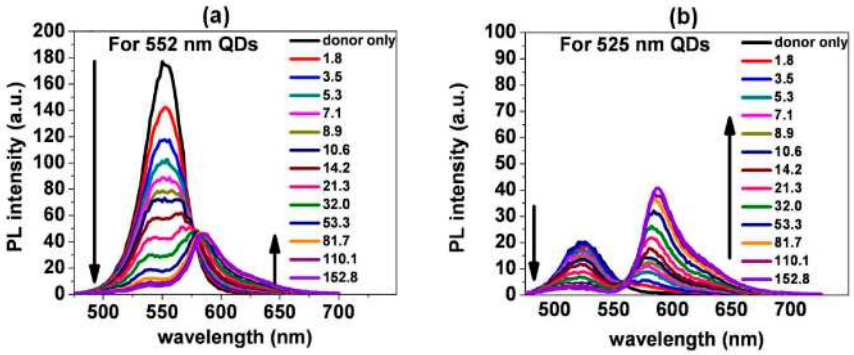

Fig. 2. SSPL spectra taken by adding controlled amounts of dye acceptors into the aqueous donor solution using CdTe quantum dots emitting at the peak wavelength of (a) 552 nm and (b) 525 nm. The legends show the corresponding A/D concentration ratios (A/D = 1.8–152.8). (Note that these PL intensity levels are measured using the same arbitrary units and that they are presented using the scales as indicated on their plots, for clear visibility.)

2.2 Time Resolved Photoluminescence (TRPL) measurements

To better understand the emission kinetics, we also performed and analyzed TRPL measurements, again by adding controlled amounts of acceptors into the aqueous donor solution (and changing A/D concentration ratios) in identical increments, both for 552 nm and 525 nm quantum dot donors. TRPL measurements were conducted using PicoQuant FluoTime 200 time resolved spectroscopy system with a fixed laser diode head at 375 nm wavelength having pulse widths of <70 ps . Figure 3 shows the evolution of photon count decay over time, parameterized with respect to the varied A/D concentration ratios, using 552 nm emitting quantum dots (given in Fig. 3a) and 525 nm emitting ones (given in Fig. 3b) at the corresponding donor emission wavelengths. Each decay curve is also shown together with its corresponding numerical exponential fits, which exhibit good fitting to the experimental data. These measurements and numerical analyses are performed at the corresponding peak emission wavelengths of the donor nanocrystals since there is an insignificant overlap between the donor and acceptor emission spectra at these peak wavelengths (Fig. 1b), which makes the analysis safe (with no detectable crosstalk between the emission of donor and acceptor molecules). The comparison of their donor photoluminescence decay lifetimes is also presented as a function of A/D concentration ratio in Fig. 3c. Here we clearly observe increasingly faster photoluminescence decay of donors. We also see that the donor lifetimes diverge away more from the starting baseline of only donors and are shortened further more for 552 nm emitting quantum dots (with its lifetimes modified from 25.3 ns to 7.2 ns) than those of 525 nm dots (with its lifetimes modified from 20.4 ns to 7.1 ns). This is because 552 nm emitting CdTe quantum dots are better optimized to match Rhodomine dye molecules and thus serve as better light-harvesting antennas to these dyes.

#124054 - $15.00 USD Received 9 Feb 2010; revised 23 Apr 2010; accepted 28 Apr 2010; published 7 May 2010

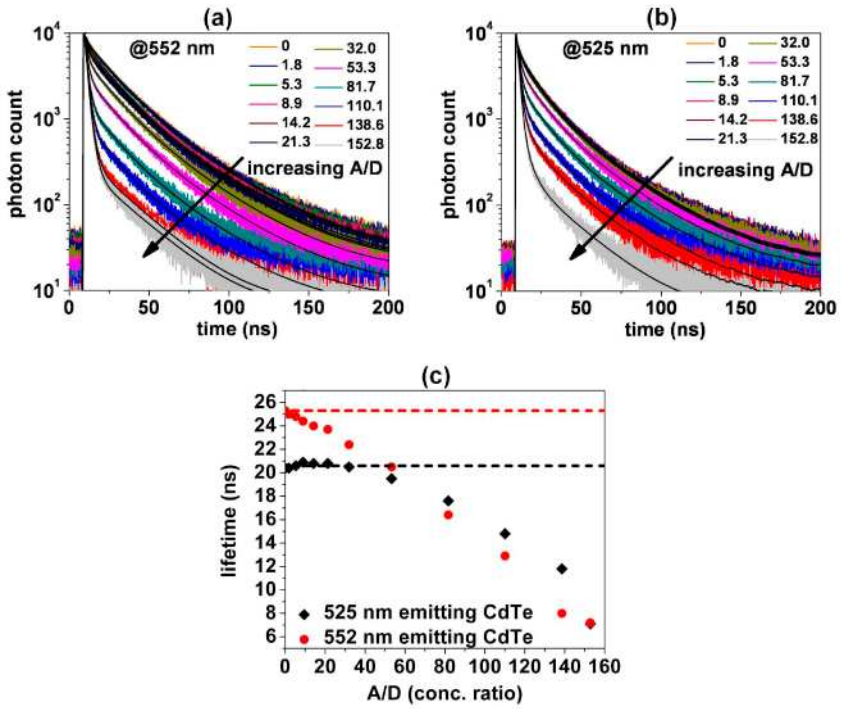

Fig. 3. TRPL measurements of donor molecules taken by adding controlled amounts of dye acceptors into the aqueous donor solution, using CdTe quantum dots emitting at the peak wavelength of (a) 552 nm and (b) 525 nm, all shown together with their corresponding numerical fits, and along with a comparative analysis of the donor photoluminescence decay lifetimes both for 552 and 525 nm emitting dots as a function of A/D concentration ratio (c). In the last plot, the red (black) dotted baseline represents the lifetime of only donors of 552 nm (525 nm) emitting dots, without any acceptors in the mixture.

Furthermore, we also performed TRPL characterization and analyses at the acceptor emission wavelengths. The peak emission wavelength of the acceptor is 581 nm, where there is a weak tail component of the donor emission. Therefore, in addition to the peak wavelength 581 nm, we performed all of the measurements and lifetime analyses also at 605 nm where there is no detectable donor emission, for safe comparison. This allowed us to make sure the effect of this tail overlap of the donor is insignificant. The evolution of photon count lifetimes at 581 nm and 605 nm are given as a function of time together with their numerical fits for 552 nm emitting quantum dots in Fig. 4a and for 525 nm emitting quantum dots in Fig. 4b. Both of their comparative lifetime analyses are given in Fig.s 4c and 4d. Due to the energy feeding as a result of FRET process, we see that the acceptor photoluminescence decay lifetimes are increased compared to the baseline of only acceptors, which is consistent with the previous literature [27, 28]. Using 552 nm emiting donors, we observe the lifetime of the acceptor molecule increases from 1.68 ns to 23.24 ns. As a function of the increasing A/D concentration ratio, since the rate of the enhancement on the emission of acceptor molecule decreases for larger A/D (Fig. 5b), the modifed lifetimes also converge towards the baseline. Regardless of the analyses conducted at either of the wavelengths (581 nm or 605 nm), we observe the same trend of the acceptor lifetime modifications, again with a stronger modification for the better optimized light-harvesting 552 nm emitting CdTe quantum dots in these experiments. All of the lifetime analysis results are also listed in Table 1-VII along with their amplitudes A_i and χ^2, chi-square values. The intensity weigted lifetime, τ_{int} is calculated through Eq. (2)

$$\tau_{\text{int}} = \sum_i A_i \tau_i^2 / \sum_i A_i \tau_i \qquad (2)$$

#124054 - $15.00 USD Received 9 Feb 2010; revised 23 Apr 2010; accepted 28 Apr 2010; published 7 May 2010

whereas the amplitude wighted lifetime, τ_{amp} is calculated using Eq. (3).

$$\tau_{amp} = \sum_i A_i \tau_i / \sum_i A_i \quad (3)$$

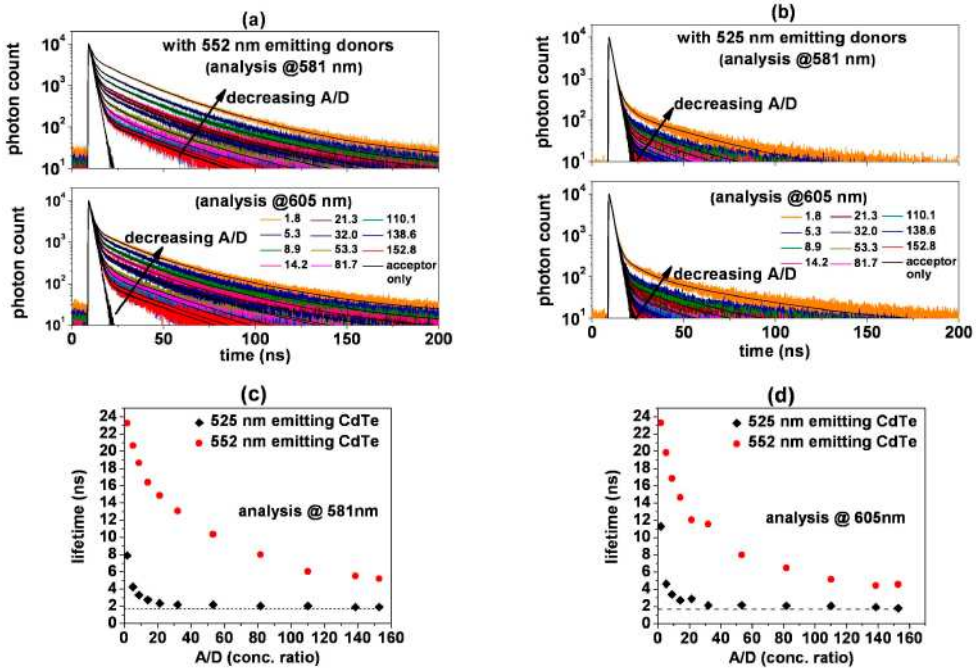

Fig. 4. TRPL measurements of acceptor molecules while varying the A/D concentration ratio, shown along with their numerical fits using (a) 552 nm and (b) 525 nm emitting quantum dots and comparative analysis of the acceptor photoluminescence decay lifetimes for emission (c) at 581 nm (acceptor peak with a weak donor tail) and (d) at 605 nm (strong acceptor tail with no donor tail as a function of A/D concentration ratios. In both plots, the dashed baseline represents the lifetime of only acceptors without any donors.

Table 1. TRPL measurement analysis (at 525 nm) of the 525 nm emitting donors varying the A/D concentration ratio.

TRPL analysis of 525 nm emitting dots at 525 nm with respect to changing A/D										
A/D	A_1	τ_1(ns)	A_2	τ_2(ns)	A_3	τ_3(ns)	τ_{int}(ns)	τ_{amp}(ns)	Eff %	χ^2
0	2341	29.32	4753	10.09	7438	0.84	20.36	8.46	0	1.25
1.8	2334	29.32	4667	9.99	7754	0.80	20.42	8.22	2.80	1.26
5.3	2367	29.52	4631	10.15	7427	0.88	20.63	8.55	–1.17	1.24
8.9	2357	29.78	4452	10.14	7504	0.91	20.91	8.54	–0.97	1.22
14.2	2328	29.78	4436	10.23	7513	0.98	20.78	8.55	–1.07	1.23
21.3	2221	30.08	4212	10.44	7725	1.06	20.82	8.40	0.64	1.21
32.0	2073	30.12	4059	10.65	7618	1.21	20.48	8.35	1.19	1.20
53.3	1541	30.46	3040	10.96	9284	1.37	19.48	6.71	20.65	1.15
81.7	1023	30.70	1985	10.96	11229	1.48	17.59	4.90	42.01	1.20
110.1	720	29.36	1248	9.56	12322	1.51	14.76	3.62	57.22	1.22
138.6	556	27.19	10004	6.93	12980	1.50	11.77	2.85	66.26	1.20
152.8	247	25.69	963	4.77	13079	1.43	7.14	2.07	75.50	1.22

#124054 - $15.00 USD Received 9 Feb 2010; revised 23 Apr 2010; accepted 28 Apr 2010; published 7 May 2010

Table 2. TRPL measurement analysis (at 581 nm) of the 525 nm emitting donors varying the A/D concentration ratio.

TRPL analysis of 525 nm emitting dots at 581 nm with respect to changing A/D								
A/D	A_1	τ_1(ns)	A_2	τ_2(ns)	A_3	τ_3(ns)	τ_{int}(ns)	χ^2
1.8	177	31.96	1037	4.33	13648	1.35	7.88	1.20
5.3	108	25.46	4150	2.34	10953	1.17	4.25	1.11
8.9	85	22.51	6648	2.05	8545	1.03	3.30	1.09
14.2	61	21.51	7053	2.02	8142	1.02	2.74	1.03
21.3	53	18.52	8478	1.92	6934	0.93	2.34	1.18
32.0	42	18.33	8653	1.92	6712	0.91	2.19	1.14
53.3	45	17.89	8789	1.90	6729	0.91	2.19	1.16
81.7	39	16.05	9252	1.88	6092	0.86	2.03	1.19
110.1	27	18.97	8715	1.92	6689	0.93	2.03	1.20
138.6	26	15.15	9299	1.90	6109	0.87	1.89	1.15
152.8	12	24.03	9177	1.86	6236	0.90	1.90	1.36

Table 3. TRPL measurement analysis (at 605 nm) of the 525 nm emitting donors varying the A/D concentration ratio.

TRPL analysis of 525 nm emitting dots at 605 nm with respect to changing A/D								
A/D	A_1	τ_1(ns)	A_2	τ_2(ns)	A_3	τ_3(ns)	τ_{int}(ns)	χ^2
1.8	128	46.63	404	9.03	14116	1.46	11.29	1.16
5.3	117	26.16	5379	2.23	9774	1.07	4.62	1.17
8.9	98	21.87	7350	2.02	7983	0.99	3.39	1.19
14.2	51	23.24	7585	2.00	7815	0.98	2.73	1.07
21.3	57	23.50	7200	2.05	8094	1.02	2.88	1.06
32.0	44	16.98	8977	1.93	6397	0.90	2.15	1.23
53.3	45	17.29	8895	1.90	6614	0.86	2.16	1.22
81.7	38	17.00	9089	1.92	6397	0.88	2.09	1.21
110.1	29	18.90	9230	1.91	6061	0.88	2.07	1.20
138.6	27	15.80	9512	1.89	5789	0.83	1.92	1.25
152.8	13	17.37	9138	1.86	6186	0.88	1.79	1.18

Table 4. TRPL measurement analysis (at 552 nm) of the 552 nm emitting donors varying the A/D concentration ratio.

TRPL analysis of 552 nm emitting dots at 552 nm with respect to changing A/D										
A/D	A_1	τ_1(ns)	A_2	τ_2(ns)	A_3	T_3(ns)	τ_{int}(ns)	τ_{amp}(ns)	Eff. %	χ^2
0	2524	36.75	6271	15.85	4265	1.26	25.26	1.12	0	1.12
1.8	2605	35.90	6016	15.61	4662	1.21	25.02	1.13	3.90	1.13
5.3	1572	41.03	6062	15.95	5216	1.57	24.81	1.17	12.83	1.17
8.9	2151	35.78	4973	15.35	6317	1.27	24.40	1.14	20.63	1.14
14.2	2212	34.70	4567	14.76	6742	1.32	23.99	1.11	25.14	1.11
21.3	2063	34.85	4498	14.92	6827	1.42	23.67	1.12	26.55	1.12
32.0	1561	34.80	3657	14.87	8501	1.46	22.44	1.14	41.63	1.14
53.3	967	35.42	2418	14.83	10387	1.56	20.51	1.13	58.55	1.13
81.7	521	34.78	1201	13.95	12215	1.62	16.38	1.15	74.03	1.15
110.1	320	34.61	720	12.74	13095	1.63	12.86	1.17	80.54	1.17
138.6	348	25.09	3560	2.78	10949	1.33	8.01	1.23	85.23	1.23
152.8	269	25.79	4194	2.65	10499	1.28	7.16	1.15	86.08	1.15

#124054 - $15.00 USD Received 9 Feb 2010; revised 23 Apr 2010; accepted 28 Apr 2010; published 7 May 2010

Table 5. TRPL measurement analysis (at 581 nm) of the 552 nm emitting donors varying the A/D concentration ratio.

TRPL analysis of 552 nm emitting dots at 581 nm with respect to changing A/D								
A/D	A_1	τ_1(ns)	A_2	τ_2(ns)	A_3	τ_3(ns)	τ_{int}(ns)	χ^2
1.8	1566	35.80	3515	15.18	8940	1.41	23.23	1.12
5.3	1042	34.53	2124	14.24	10977	1.44	20.67	1.10
8.9	774	34.15	1518	13.53	12159	1.46	18.64	1.12
14.2	508	34.86	1080	13.33	12809	1.48	16.38	1.16
21.3	486	32.94	913	12.23	13030	1.50	14.85	1.12
32.0	425	31.51	755	10.77	13304	1.49	13.05	1.14
53.3	278	31.41	543	9.88	13606	1.51	10.36	1.14
81.7	237	28.43	568	6.27	13723	1.48	7.96	1.12
110.1	209	25.08	4409	2.48	10629	1.18	6.05	1.05
138.6	181	24.82	5258	2.32	9634	1.13	5.51	1.06
152.8	167	24.72	4266	2.44	10793	1.19	5.22	1.05

Table 6. TRPL measurement analysis (at 605 nm) of the 552 nm emitting donors varying the A/D concentration ratio

TRPL analysis of 552 nm emitting dots at 605 nm with respect to changing A/D								
A/D	A_1	τ_1(ns)	A_2	τ_2(ns)	A_3	τ_3(ns)	τ_{int}(ns)	χ^2
1.8	701	42.56	1591	15.37	11970	1.46	23.28	1.13
5.3	548	40.07	1320	14.82	12481	1.51	19.85	1.11
8.9	478	36.82	971	13.21	13060	1.52	16.85	1.15
14.2	342	37.02	763	13.08	13383	1.53	14.63	1.14
21.3	306	33.70	594	10.39	13481	1.50	12.05	1.14
32.0	300	33.09	596	10.16	13407	1.53	11.55	1.17
53.3	255	27.88	897	4.70	13627	1.43	7.99	1.10
81.7	225	25.53	3185	2.73	11804	1.26	6.47	1.09
110.1	161	24.90	5866	2.28	9180	1.11	5.13	1.05
138.6	134	23.86	6681	2.16	8412	1.04	4.42	1.08
152.8	119	25.71	5840	2.25	9138	1.09	4.55	0.98

Table 7. TRPL measurement analysis (at 581 and 605 nm) of the 581 nm emitting acceptors varying the A/D concentration ratio.

TRPL analysis of 581 nm emitting Rhodamine B molecules at 581 nm							
A_1	τ_1(ns)	A_2	τ_2(ns)	A_3	τ_3(ns)	τ_{int}(ns)	χ^2
–17	0.001	8277	1.98	7105	1.006	1.68	1.88
TRPL analysis of 581 nm emitting Rhodamine B molecules at 605 nm							
A_1	τ_1(ns)	A_2	τ_2(ns)	A_3	τ_3(ns)	τ_{int}(ns)	χ^2
10225	1.89	25883	0.53	–22115	0.45	1.69	1.23

2.3 Light harvesting analyses and remarks

Fig.s 3 and 4 demonstrate clearly the effect of Förster radius on the lifetime modifications of the donor and acceptor molecules. For further analyses, we also calculate energy transfer efficiency and light harvesting enhancement of the acceptor emission. The energy transfer efficiency is extracted from the amplitude weighted donor lifetime, τ_{amp} in the presence and absence of the acceptor molecules using Eq. (4)

$$\eta_{FRET} = 1 - \frac{\tau_{DA}}{\tau_D}. \quad (4)$$

#124054 - $15.00 USD Received 9 Feb 2010; revised 23 Apr 2010; accepted 28 Apr 2010; published 7 May 2010

Here τ_{DA} is the ampitude weighted lifetime of donors in the presence of acceptors and τ_D is that of donors in the absence of acceptors [26].

Figure 5a reveals the comparison of efficiency levels extracted from TRPL measurements. Here we observe that the energy transfer efficiency increases with the increased A/D concentration ratio, as the donors find more acceptors around them to transfer more of their excitation energy. Tuning the A/D concentration ratios and using better optimized 552 nm emitting quantum dot donors, we observe a maximum energy transfer efficiency of 86%, which is obtained at an A/D concentration ratio of 152.8 in our experiments. This comparison shows that the efficiency levels are higher using 552 nm emitting quantum dots than those of 525 nm emitting ones.

To show the effect of nonradiative energy transfer mediated light harvesting on the emission enhancement of the acceptor molecules, we further compute the light-harvesting factor for the acceptor emission (Fig. 5b). These calculations are carried out through fitting SSPL measurements (in Fig. 2) of the donor quantum dots to a Gaussian distribution and comparing the overall emission (donor + acceptor mixture) with the emission of only acceptors (corresponding to the same concentration of acceptor molecules used in each A/D concentration point). In these calculations, the tail overlap of the donor emission on the acceptor emission is also considered, and any possible contribution from the tail (although weak) is also subtracted. Here we observe that the relative enhancement factor of the acceptor emission is decreased with the increased A/D concentration ratio, because the acceptors increasing in number find fewer donors around them to be fed via nonradiative energy transfer, which indicates a tradeoff between the efficiency and light harvesting factor.

Also, we again observe that 552 nm emitting aqueous CdTe quantum dots are better light-harvesting antennas in water for Rhodamine B dye molecules in comparison to those quantum dots emitting at 525 nm. In the light of these experiments and analyses, such light harvesting is possible; however, one needs to consider the tradeoff between efficiency and enhancement factor to choose an operating point. These results also indicate that nonradiative energy transfer assisted light harvesting may enable quantum dot multiplexed dye biodetection systems, on which we are currently working.

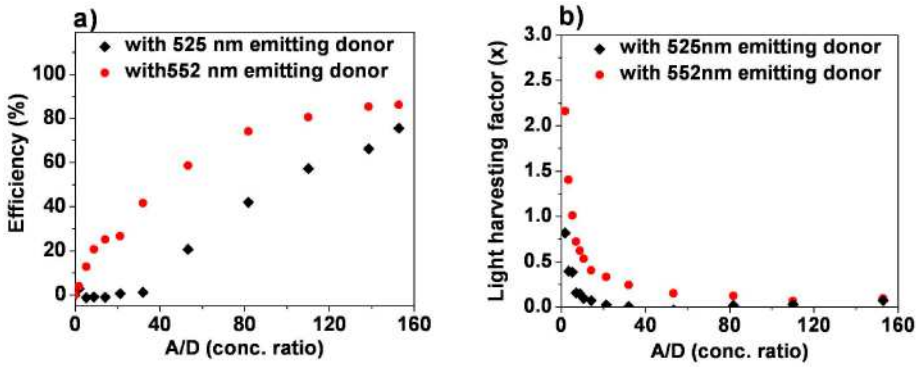

Fig. 5. Comparison of (a) FRET efficiencies and (b) enhancement of the acceptor emission, using 552 nm and 525 nm emitting CdTe quantum dot donors, as a function of the A/D concentration ratio.

3. Conclusion

In conclusion, as a proof-of-concept demonstration, we have presented nonradiative energy transfer based light harvesting of aqueous colloidal CdTe quantum dot antennas for dye molecules in water. Our experiments show that these quantum dots used as donors need to be carefully optimized to match Rhodamine B used as acceptors. In our experiments, we have observed strong lifetime modifications of these CdTe quantum dots from 25.3 to 7.2 ns. We have demonstrated the energy transfer efficiency tuning up to 86% as the acceptor-donor

#124054 - $15.00 USD Received 9 Feb 2010; revised 23 Apr 2010; accepted 28 Apr 2010; published 7 May 2010

concentration ratio is varied. These experiments indicate that nonradiative energy transfer mediated light harvesting using aqueous quantum dots leads to enhanced emission of dye molecules in water at wavelengths beyond the absorption range of the dyes. One should also note that a good operating point in the A/D concentration ratio for a specific donor-acceptor pair has to be set to provide both reasonably high efficiency and high light harvesting of the acceptor emission. This nonradiative energy transfer assisted light harvesting holds great potential for future quantum dot multiplexed biological and optoelectronic applications.

Acknowledgements

This work is supported by EU-FP7 Nanophotonics4Energy NoE, BMBF TUR 09/001, and TUBITAK EEEAG 106E020, 107E297, 107E088, 109E002, and 109E004. HVD acknowledges support from ESF-EURYI and TUBA-GEBIP, and EM, from TUBITAK-BIDEB.

#124054 - $15.00 USD Received 9 Feb 2010; revised 23 Apr 2010; accepted 28 Apr 2010; published 7 May 2010